Techno-Science Research Journal V13 (2) (2025) P 68-78

Content list available at ITC

Techno-Science Research Journal

Journal Homepage: http://techno-srj.itc.edu.kh/

Techno-Science Research Journal

Economic Study on Integrating PV-DG with Grid-Tie: Case Study in Cambodia

Daravann Mel[1*], Sokchea Am[2], Phok Chrin[2]

[1] *Research and Innovation Center, Institute of Technology of Cambodia, Russian Federation Blvd., P.O. Box 86, Phnom Penh, Cambodia*

[2] *Department of Electrical and Energy Engineering, Faculty of Electrical Engineering, Institute of Technology of Cambodia, Russian Federation Blvd., P.O. Box 86, Phnom Penh, Cambodia*

Received: 12 August 2024; Revised: 07 October 2024; Accepted: 11 October 2024; Available online: 31 August 2025

Abstract: *The growing yearly power demand caused by population increases and economic upswings results in considerable energy losses and voltage instability in the distribution system. This study proposes integrating photovoltaic distributed generation (PV-DG) with the battery system (BS) into the grid to address these issues. Despite the many benefits of PV-DG and BS, improper placement can negatively impact the distribution network's technological aspects. The goal of this study is to enhance the production of grid-tied PV-DG and BS along the distribution network. Firstly, using particle swarm optimization (PSO), the study examines two scenarios according to the grid and general condition of PV-DG constraint to determine the optimal placement and size for the PV-DG system. Next, the BS is utilized to store surplus energy from PV-DG and to supply it back into the grid during peak hour (20:00). The backward-forward sweep (BFS) method analyzes 24-hour energy loss and voltage profiles for each scenario. The 22kV radial feeder of 115/22kV grid substation Osaom in Pursat, Cambodia, is used as a case study. The simulation results demonstrated the optimum location was bus-24, and capacity for PV-DG and BS were 2.34248 MW and 1.243 MWh, respectively, within the loss reduction per year of 19.56% from 1,115.8674 MWh loss (system without proposed method) and acceptable voltage levels of 0.95 p.u to 1.05 p.u. Finally, during the 20-year planning study and purchasing cost of energy (COE) of 0.157 USD/kWh for economic evaluation, scenario 1 was a preferable case in which the project was fully refunded in short periods of 7.75 and 13.12 years of simple payback period (SSP) and discounted payback period (DPP), respectively, with a total profit of 558,396.434 USD of net present worth (NPW). In short, these results demonstrated the advantages of employing the proposed method to create the efficient and dependable MVAC distribution system in Cambodia.*

Keywords: Photovoltaic-distributed generation; battery storage; power loss minization; techno-economic analysis; Cambodia

1. INTRODUCTION

To meet the rising need for electricity as a result of economic expansion, Cambodia's government has approved the development of both non-renewable and renewable energy sources under its Power Development Master Plan (PDP), which runs from 2022 to 2040 [1]. Solar PV and battery systems play important roles in the power industry and are developing as crucial low-carbon technologies. The integration of PV systems into the grid offers issues such as energy loss, voltage fluctuations, and feeder capacity, particularly in low voltage (LV) networks [2]. Comparing conventional networks to modern distribution networks that use renewable energy sources may assist reduce system loss and voltage drop.

One of the most significant issues faced by PV systems is the fluctuation of global horizontal irradiance (GHI) and unexpected cloud cover, which causes the PV system to generate less power than its maximum power point (MPP). As a result, the amount of electricity pumped into the grid is lower than predicted, causing voltage dips. To address this issue, many ways have been proposed, including inveter-based reactive power of PV systems [3] and voltage regulation from utility sources [4]. According to [5], incorporating energy storage technologies, such as battery energy storage (BES), has been considered as a way to reduce voltage fluctuations. However, customer-controlled BES may not comply with grid code requirements and may not be economically viable for users without utility cooperation.

This paper presents a strategy for stabilizing the voltage profile and minimizing energy loss by combining PV-DG with the BS, with an emphasis on utility. For the suggested system to be installed, this strategy requires utility support. The research proposes optimizing the location and dimension of the proposed system using PSO for two scenarios, taking into account economic indicators over a 20-year timeframe. Two

[*] Corresponding author: Daravann MEL
E-mail: mel_daravann@gsc.itc.edu.kh; Tel: +855-12 436 997

comparative scenarios are provided to assess the impact of integrating proposed technologies with the grid as well as the techno-economic viability, which has not previously been studied in prior research. The MATLAB/Simulink application is used to simulate the PSO and BFS power flow codes. This concept may be of interest to utilities as an alternative to traditional approaches.

This papper was divided into four sections. First, an introduction is provided. Section 2 then describes the suggested technique, which includes thorough explanations, simple scenarios, flowcharts, and a case study. Section 3 describes the simulation result and their consequences. Finally, section 4 summarizes the result and suggests directions for further research.

2. METHODOLOGY

2.1 Research work

In the MVAC system, the algorithms select the ideal PV-DG location at random A flowchart was utilized to examine PV-DG integration with the BS, assessing technology and finance for successful investments. Two scenarios, such as the utility and the general condition of PV-DG size constraints, were investigated. Fig. 1 depicts a full flowchart analysis.

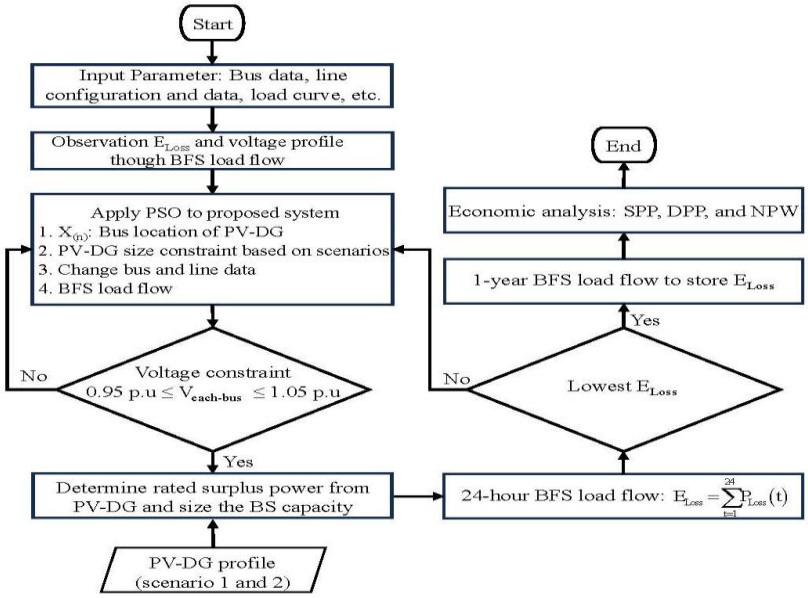

Fig. 1. The overall flow chart for proposed method

- Step 1: Feed in line data, line configuration, bus data, load curve, and economic data. Conduct a 24-hour power flow analysis using BFS to observe the voltage profile and power loss of the system.
- Step 2: PSO is utilized to find out the optimal location and peak power of PV-DG according to the objective function of minimizing power loss and voltage constraints. The sizing of PV-DG follows the conditions of scenarios 1 and 2.
- Step 3: Each scenario means that PV-DG is integrated with the grid to supply power to the system. When power from PV-DG is used to meet excess load demand, the battery is used as the reservoir to store energy and supply it back into the grid during peak hours.
- Step 4: Determine the rated surplus power from PV-DG at a specific time for the whole year to size of the BS capacity. The BS is installed at the same location as PV-DG in terms of fast response supply and load-shedding.
- Step 5: Utilize BFS power flow for 24-hour power to decide the lowest energy loss in each scenario.
- Step 6: 20-year BFS power flow to store energy loss. Moreover, compute the business aspects for NPW, SPP, and DPP over the study period of 20 years.
- Step 7: Finally, compare the result outcome of both the technical aspect and the business indicator of each scenario to the based-case.

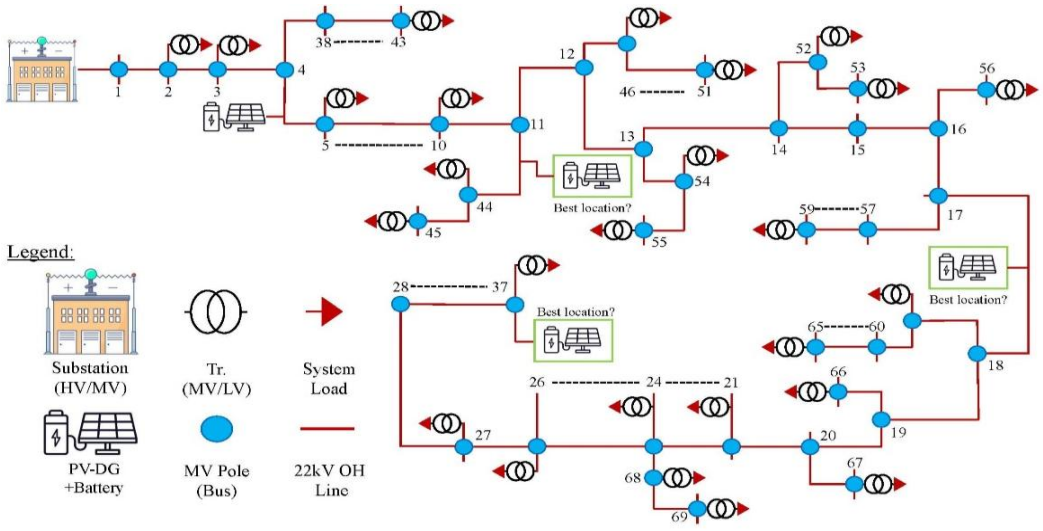

Fig. 2. Radial topology of radial feeder for each scenario

Fig. 2 shows the proposed radial topology netowrk for each scenario. The PSO simulation results reveal the the optimum location and power of PV-DG.The surplus power from PV-DG is stored in BS to prevent reverse power flow into the substation during low power demand times. On 20:00, the BS return stored power to the grid. When PV-DG and the BS are absent, the system load takes power from the substation.

2.2 Objective function and constraint

In this paper, the objective function focuses on reducing energy loss for 24-hours and is exposed to the constraints of each bus voltage along the MV network, as mentioned in the researched study [6]. The utility [7] and general condition [8] of the PV-DG size constraint are represented in (Eq. 3 and 4), respectively.

- Objective function: $\min\left[\sum_{t=1}^{24h} P_{Loss}(t)\right]$ (Eq. 1)
- Constraint:

$$0.95\,p.u \leq V_{each\_bus} \leq 1.05\,p.u \quad [6] \quad \text{(Eq. 2)}$$

$$P_{min,grid} \leq P_{PV-DG} \leq 0.5P_{max,grid} \quad [7] \quad \text{(Eq. 3)}$$

$$P_{min,grid} \leq P_{PV-DG} \leq P_{max,grid} \quad [8] \quad \text{(Eq. 4)}$$

2.3 Design concept of PV-DG and BS ability

2.3.1 PV array capacity computation

The size of the solar panel and the amount of solar irradiation are both important factors in determining the power output of a PV-DG system. Furthermore, the temperature at the chosen location influences overall performance [9]. The PV array's rated capacity (kW) is shown in (Eq. 5). According to [10], the working temperature of solar PV modules was calculated in (Eq. 6).

$$Y_{PV} = \frac{P_P}{f_P\left(\frac{G_T}{G_{T,STC}}\right)\left[1+\alpha_P\left(T_C - T_{C,STC}\right)\right]} \quad \text{(Eq. 5)}$$

$$T_C = T_{air} + (NOCT - 20)\left(\frac{G_T}{0.8}\right) \quad \text{(Eq. 6)}$$

Where :

P_P = Powr requirement or peak output power PV (kW)
F_P = Derating factor of solar PV panel (%)
G_T = Solar irradiation data at current time (kW/m^2)
$G_{T,STC}$ = Solar irradiation data at STC (kW/m^2)
α_P = Temperature coefficient of power (%)
T_C = Temperature data for current time (^{o}C)
$T_{C,STC}$ = Temperature data for STC (^{o}C)
T_{air} = Air ambient temperature (^{o}C)
NOCT = Norminal operating temperature of PV (^{o}C)

The derating factor for the solar PV system decreased the power output of the PV array due to the efficiency of the PV module, PV inverter, AC-DC wiring loss, soiling, shading, etc. In [11], [12], [13], the derating factor was 0.85%, 0.88%, and 90%, respectively. Thus, the 90% value is selected in the study.

Air ambient temperature is the key factor that also effects solar PV output based on the location of solar PV system

installation. According to the observed annual average mean surface air temperature of Cambodia (Pursat) for 1901~2022 by the Climatic Research Unit (CRU) in [14], the 2022 annual mean air temperature of 26.85 ^{o}C is used in (Eq. 6). Moreover, solar radiation at the current time, which corresponds to the air ambient temperature of 26.85 ^{o}C in 2022, is 0.973 kW/m^2, according to [15].

2.3.2 Battery system capacity computation

The battery's cell arrangement is used for the battery system to store surplus energy form P_P at the specific time period, depth of discharge and roundtrip efficiency [9]. The BS size (B_{Size}) or capacity is calculated in (Eq. 7).

$$B_{Size} = \frac{P_B \, x \, T_{RP}}{DOD \, x \, \eta_{Battery}} \qquad \text{(Eq. 7)}$$

Where :

T_{RP} = Time required period to supply power (hrs)
P_B = Power required or rated stored power (kW)
DoD = Depth of discharge for battery (%)
$\eta_{Battery}$ = Battery roundtrip efficiency (%)

2.4 Economic analysis

2.4.1 Core parameter formulations for NPW, SPP, and DPP

From 2010 to 2022, the global total installation cost for solar PV systems has significantly fallen from 5,124 to 876 USD/kW [16]. As a result, the following equation (Eq. 8) is based on the installation cost per unit (IC_P) of 876 USD/kW.

Similar to solar PV, Li-on battery system installation costs are expected to decrease by 393-581 USD/kWh in 2018 and 308-419 USD/kWh by 2025 [17]. This study, followed by the technical assistance consultant's report [18], estimates the installation cost of the whole BS at 348 USD/kWh. The total investment cost ($I_{P\&B}$) for PV-DG with the BS system is computed using the calculation equation below.

$$I_{P\&B} = \left(IC_B \, x \, B_{Size}\right) + \left(IC_P \, x \, Y_{PV}\right) \qquad \text{(Eq. 8)}$$

Where :

IC_P = Installation cost per unit for PV (USD/kW)
IC_B = Installation cost per unit for battery (USD/kWh)
B_{Size} = The battery system capacity (kWh)

Earnings before tax (EBT) are the annual revenues obtained by selling power from the PV-DG with battery system to the grid. The EBT is determined by the purchase of COE as well as the operating and maintenance costs (OM). The COE of 0.157 USD/kWh, which is the mean value of the highest purchase cost of electricity, 0.09 USD/kWh [19], and the lowest levelized cost of storage, 0.225 USD/kWh [20], is chosen for the case study. Furthermore, in [21] and [22], the OM for PV-DG and the battery are set at 20 USD/kW and 4.59 USD/kWh, respectively. EBT for PV-DG with the battery is calculated using the following equation:.

$$EBT = COE\left(E_P + E_B\right) - \left(OM_P + OM_B\right) \text{ (Eq. 9)}$$

Where :

E_P = Annual energy from PV-DG (kWh)
E_B = Annual energy from battery (kWh)
OM_P = Operation and maintenance cost of PV-DG (USD)
OM_B = Operation and maintenance cost of battery (USD)

However, all the income must be deducted according with country rules. In Cambodia, 20% [23] is the rating for all business types with a yearly income of more than 36,585.36 dollars (1USD=4,100 Riel). The EAT (USD) for PV-DG and battery is indicated in the following equation.

$$EAT = EBT * \left(1 - 20\%\right) \qquad \text{(Eq.10)}$$

2.4.2 NPW , SPP and DPP formulation

The project was permitted if NPW was positive; nevertheless, it was denied if NPW was negative at the end of the planning study year [24]. The NPW was calculated using the equation below, which included the cash flow. In this work, cash flows are equal to EAT and the initial investment cost ($I_{P\&B}$), and the discounted rate is considered to be equal to the average 4-year (2020-2023) interest rate from the General Department of Tax [25], [26], [27], [28].

$$NPW = \sum_{i=1}^{N} \frac{CF_i}{\left(1 + DR\right)^i} - I_{P\&B} \qquad \text{(Eq. 11)}$$

Where :

CF = Annual cash flow of project or investment (USD)
DR = Discounted rate (%)
$I_{P\&B}$ = Initial investment cost for proposed system (USD)
N = Investment or project period (year)

Investing with shorter payback times is generally more appealing [24]. The SPP is represented in the following:

$$SPP = \frac{I_{P\&B}}{CF} \qquad \text{(Eq. 12)}$$

The DDP is the time it takes for the total of the uneven cash flows to match the initial cost. According to the DDP criterion, an investment is accepted if its DDP is shorter than a certain

number of number of years [24]. DPP is calculated using equation (Eq. 13).

$$DPP = \frac{\ln\left(\frac{1}{1-\frac{I_{P\&B} \times DR}{CF}}\right)}{\ln(1+DR)} \quad \text{(Eq. 13)}$$

2.5 Case study

The proposed location was conducted in a rural radial feeder of Electricité du Cambodge (EDC) grid substation called Ousaom (GS-22). The GS-22 is located at 12° 1' 25.7196" North and 103° 12' 21.4524" East.

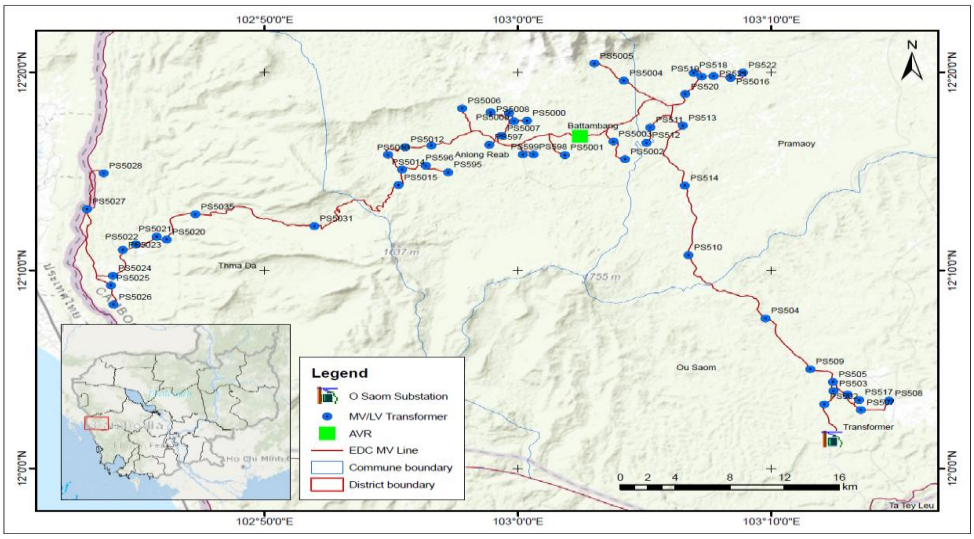

Fig. 3. Testing MV radial distribution feeder of GS-22

2.6 PV and load profile curve

The examined daily load curve was assumed by starting with the peak load demand (0.95 PF) and normalizing based on the load profile found in urban households [29]. According to the National Solar Radiation Database (NSRD) [30], GHI varies somewhat between two solar farm locations: Tmart Pong 60MW (11° 38' 19.4028" N, 104° 40' 35.5656" E) and Risen Energy 60MW (13° 9' 37.0728" N, 102° 58' 33.312" E). To determine the PV-DG power profile, power generation data from the Tmart Pong solar farm in 2020 was utilized and adjusted. In Fig. 4, the load curve and yearly average PV curve for 24 hours were visually depicted as two independent curves.. Finally, the surface air temperature was recored and obtained from CRU was illustrated in Fig. 5.

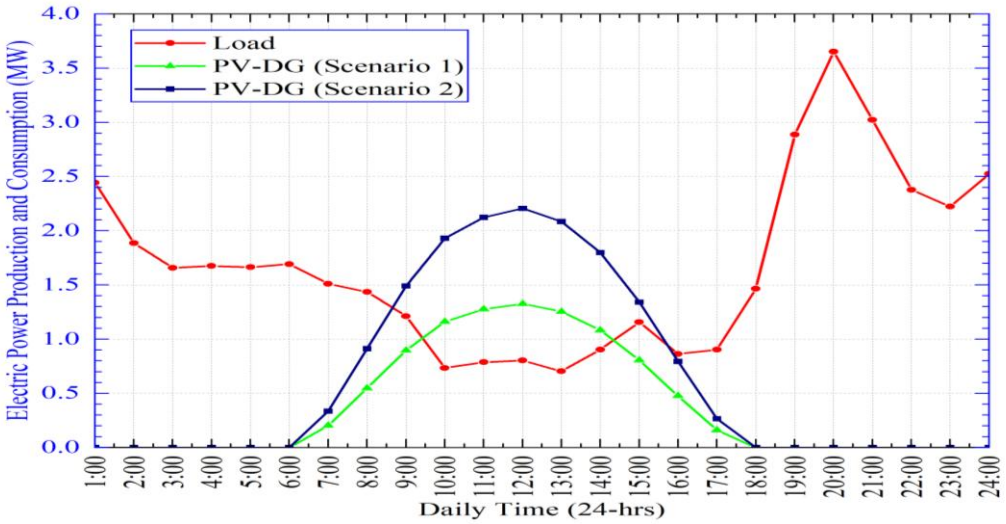

Fig. 4. Load and PV-DGs performance curve

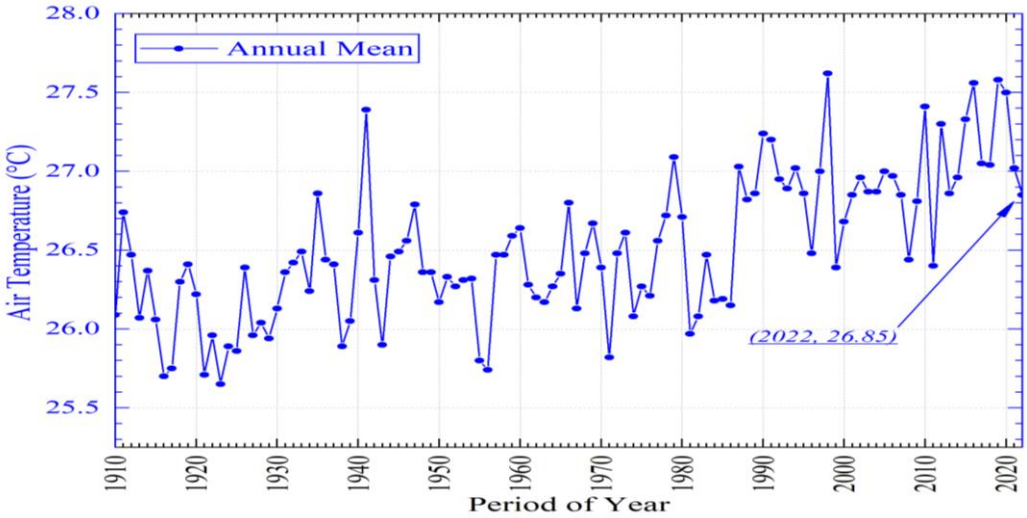

Fig. 5. Surface air temperature of Pursat from 1901-2022

3. RESULTS AND DISCUSSION

3.1 Observation result for system without scenarios

According to Fig. 6, between 19:00 to 24:00, the load absorbed a lot of electricity from the grid, which impacted system voltage profile. On 20:00, all buses had the dramatic drop in voltage (below 0.9 p.u), including buses 8, 37, and 69, which had the system's poorest voltage profile. Line loss causes the total energy loss (E_{Loss}) of 1,115.8674 MWh annually. Adding more power generation sources along the radial feeder would enhance the voltage profile and reduce power loss.

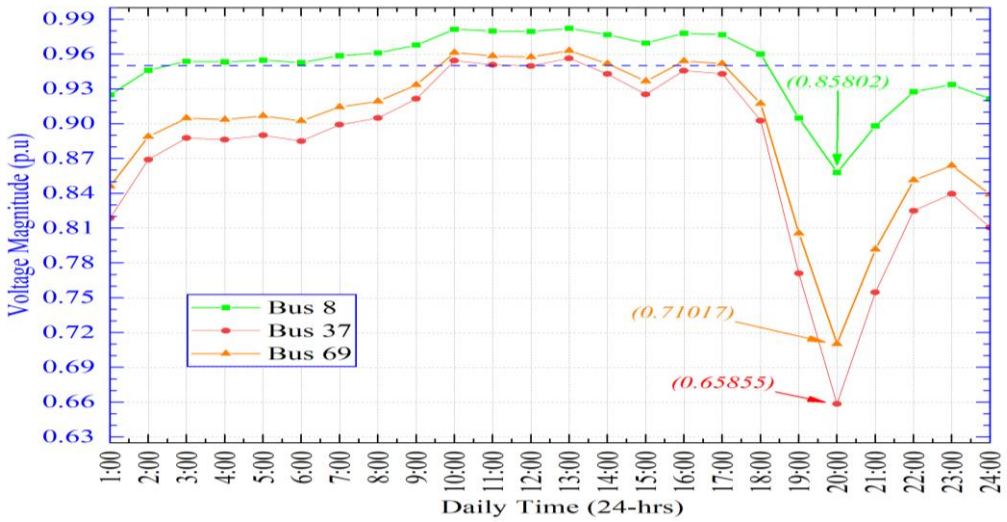

Fig. 6. Voltage curve for bus 8, 37, and 69

3.2 Result for system with scenarios 1 and 2

The results from PSO and 24-hour power flow by the BFS approach revealed the E_{Loss} (3.0572 MWh) over 24-hour period when comparing energy loss in different scenarios with the initial case, indicating bus 24 and 19 as the essential locations for adding PV-DG and the battery in each scenario. In Fig 7 and 8 show the optimal peak power and positioning of PV-DG and batteries for scenario 1 (1.8264 MW, 1.1187MWh) and scenario 2 (3.0369 MW, 2.3268 MWh).

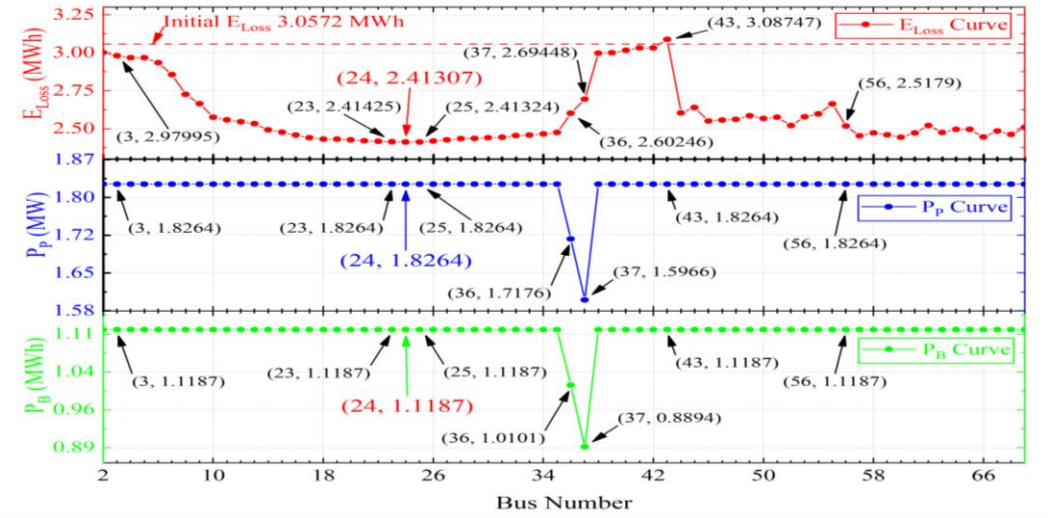

Fig. 7. The bes location and power of PV-DG, BS and the lowest 24-hour E_{Loss} in Scenario 1

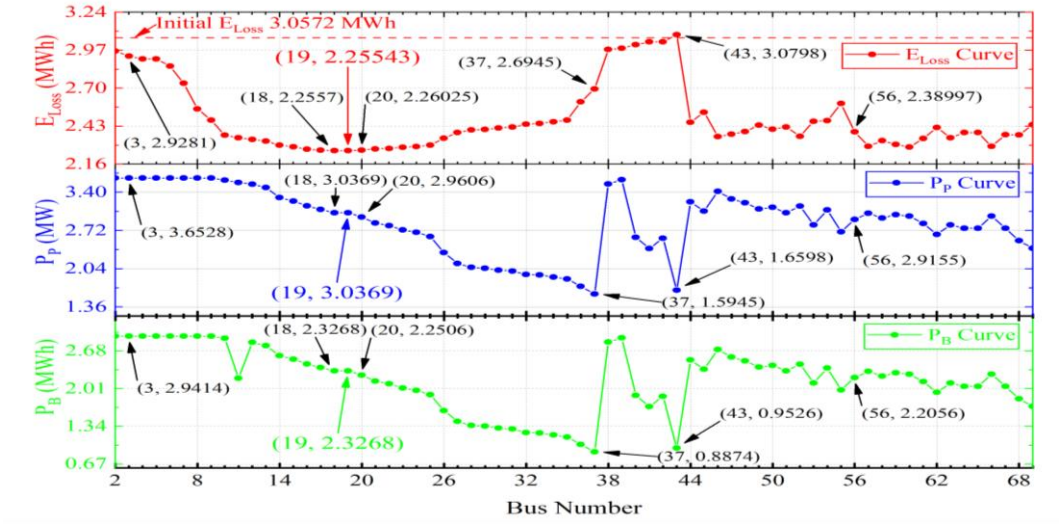

Fig. 8. The best location and power of PV-DG, BS and the lowest E_{Loss} in Scenario 2

In scenarios 1 and 2, combining PV-DG (daytime) and the battery (peak hour) results in a considerable rise in the system voltage profile. Outside of these times, voltage levels recover to their initial state when PV-DG and the battery power injection are stopped. The overall E_{Loss} for 24-hour and 1-year is 2.41307 MWh, 897.6327 MWh for scenario 1, and 2.25543 MWh, 835.3727 MWh for scenario 2. Fig. 9 and 10 also show the voltage rise for buses, with baselines 0.95 and 1.05 p.u.

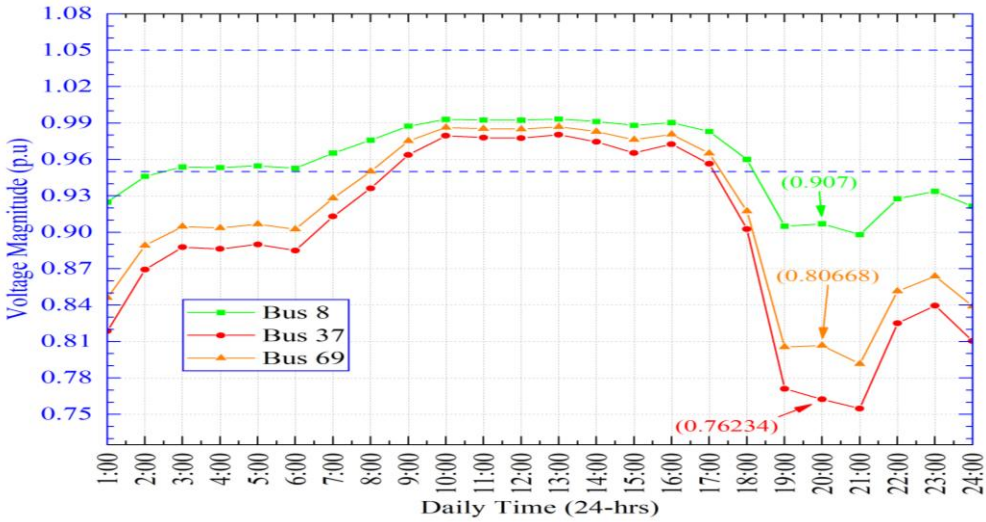

Fig. 9. Voltage curve for bus 8, 37, and 69 in scenario 1

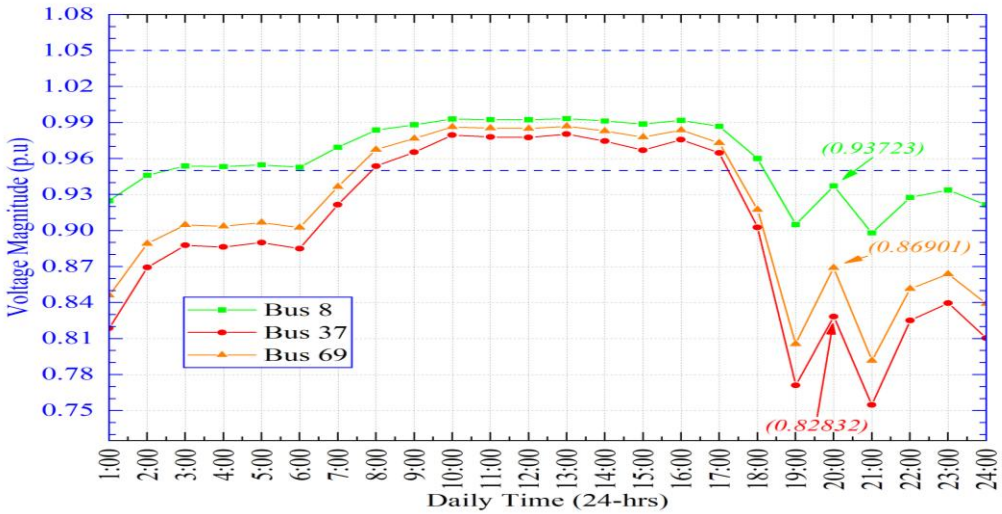

Fig. 10. Voltage curve for bus 8, 37, and 69 in Scenario 2

Table 1. Techno-eco result for system within scenarios

Items	Initial-Case	Scenario 1	Scenario 2
Optimal bus	-	24	19
P_P (MW)	-	1.8264	3.0369
Y_{PV} (MW)	-	2.34248	3.8948
P_B (MWh)	-	1.1187	2.3267
B_{Size} (MWh)	-	1.243	2.5852
V_{min} (p.u)	0.6586	0.8992	0.8992
V_{max} (p.u)	0.9969	0.9987	0.9987
E_{Loss} (MWh)	1,115.8675	897.6327	835.3727
N (Year)	-	20	20
$E_{P\&B}$ (MWh)	-	57,767.32	76,611.2452
$OM_{P\&B}$ (USD)	-	24.59	24.59
COE (USD/kWh)	-	0.157	0.157
DR (%)	-	8.465%	8.465%
$I_{P\&B}$ (USD)	-	2,484,576.48	4,311,494.4
EBT (USD)	-	400,918.4924	511,636.2069
EAT (USD)	-	320,734.794	409,308.9655
NPW (USD)	-	558,396.434	(428,173.6038)
SPP (Year)	-	7.75	10.53
DPP (Year)	-	13.12	27.35

Table 1 shows the technical achievement obtained by maintaining appropriate voltage throughout all scenarios and obtaining the lowest energy loss (E_{Loss}) in scenario 2 though the combination of PV-DG and the battery as compared to scenario 1. However, economic evaluation findings show that the project has NPW and does not require an unnecessary year of study (SPP, DPP), indicating that it should be accepted the in the research study. Therefore, according to technological and commercial aspects, scenario 1 reflects the significant topology of allotted era for research planning.

Fig. 11 depicts the cash flow, SPP, DPP, and NPW for both scenario 1 and 2. Within fixed cash flow, the investment was completely recovered after 7.75 years and had the positive NPW value (8-20 years). Similary, in 13.12 years, the investment was fully recovered (uneven cash flow) with the positive NPW value (14~20 years). Scenario 1's economic results reveal the total positive value of NPW without exceeding the investment year for SPP and DPP.

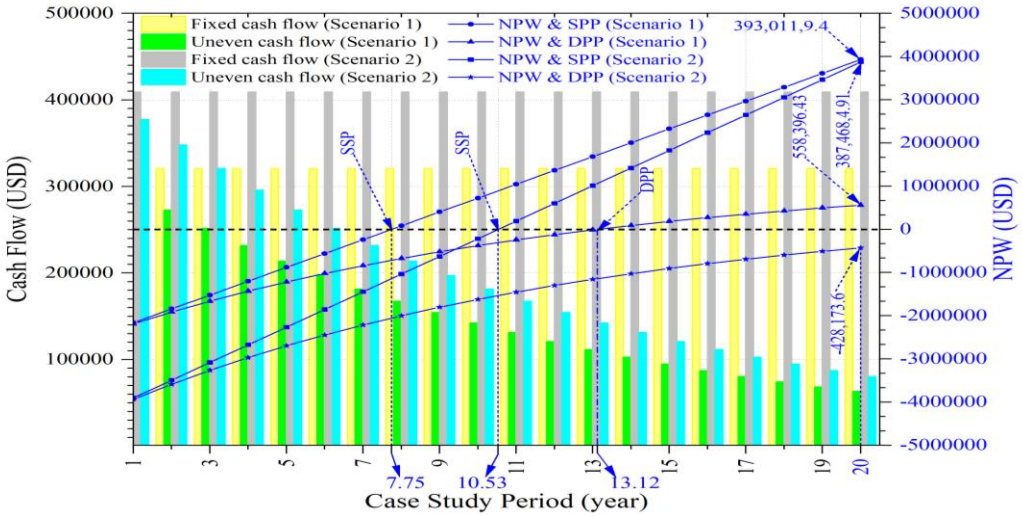

Fig. 11. Cash flow, SPP, DPP, and NPW result of each scenario

Contratry to scenario 1, in scenario 2, SPP has the completely recovered investment at 10.53 years (based on constant cash flow) and the positive NPW value from 11-20 years. However, the investor was unable to benefit (because of inconsistent cash flow) even in the twentieth year with the negative NPW value. Thus, the economic outcome of scenario 2 failed for this research study.

3.5 Discussion

The show that the initial case has the maximum energy loss (1,115.8675 MWh/year), which is mainly due to line losses. However, when PV-DG with the battery is incorporated into buses 24 and 19 according to the scenarios, the system's line losses are reduced by roughly 19.56% and 25.14% per year. Despite this decrease, the voltage drop remains similar with the baseline scenario of no power from PV-DG and the battery. In scenario 2, the technological element provided considerable benefits in terms of loss reduction and voltage stabilization. However, the business indications, notably the negative for NPW and the inability to return the investment (DPP), discouraged investors from funding the project. Thus, it is clear that scenario 1 emerged as the preferable alternative over scenario 2, delivering the greatest outcomes across both technology characteristics and business indicators as compared to the first scenario.

4. CONCLUSIONS

This describes a methodology for finding the ideal location and capacity of PV-DG and the battery system while taking into account constraints such as voltage limits, utility, and general condition-based DG size limitations. The findings of scenario 2 reveal that the MVAC distribution system under examination functions best, with losses reduced by 19.54% and 25.14% in scenarios 1 and 2 from 1,115.8675 MWh, respectively. Despite technological superiority, scenario 2 failed to deliver positive results for business indicators, which are critical for the study's decision-making process. As a consequence, scenario 1 was the better option, as the project was fully reimbursed in a short period of 7.75 and 13.12 years for SSP and DPP, respectively, with a total profit at year-end NPW of 558,396.434 USD. These findings highlight the benefits of using the suggested strategy to develop an efficient and dependable MVAC distribution system in Cambodia. Future work will include the implementation of battery charge and discharge techniques, as well as the development of fault protection systems for interaction with PV-DG and the battery system inside the topology.

REFERENCES

[1] MME, "Cambodia Power Development Master Plan 2022-2040," *Grantham Res. Inst. Clim. Change Environ. Was Establ. Lond. Sch. Econ. Polit. Sci.*, no. September, 2022.

[2] Y. Gabdullin and B. Azzopardi, "Impacts of Photovoltaics in Low-Voltage Distribution Networks: A Case Study in Malta," *Energies*, vol. 15, no. 18, 2022, doi: 10.3390/en15186731.

[3] M. J. E. Alam, K. M. Muttaqi, and D. Sutanto, "A novel approach for ramp-rate control of solar PV using energy storage to mitigate output fluctuations caused by cloud passing," *IEEE Trans. Energy Convers.*, vol. 29, no. 2, pp. 507–518, 2014, doi: 10.1109/TEC.2014.2304951.

[4] H. Sugihara, K. Yokoyama, O. Saeki, K. Tsuji, and L. Member, "Economic and Efficient Voltage Management Using.pdf," *Ieee Trans. Power Syst.*, vol. 785, pp. 1–10, 2012.

[5] M. J. E. Alam, K. M. Muttaqi, and D. Sutanto, "Mitigation of rooftop solar PV impacts and evening peak support by managing available capacity of distributed energy storage systems," *IEEE Trans. Power Syst.*, vol. 28, no. 4, pp. 3874–3884, 2013, doi: 10.1109/TPWRS.2013.2259269.

[6] and B. R. C. Chhlonh, M. C. Alvarez-Herault, V. Vai, "Comparative Planning of LVAC for Microgrid Topologies With PV-Storage in Rural Areas - Cases Study in Cambodia," *IEEE PES Innov. Smart Grid Technol. Conf. Eur.*, 2022, doi: 10.1109/ISGT-Europe54678.2022.9960511.

[7] EAC, "regulation-general-conditions-for-connecting-SolarPV-kh.pdf," 2018, *Electricity Authority of Cambodia*.

[8] P. Prakash and D. K. Khatod, "Optimal sizing and siting techniques for distributed generation in distribution systems: A review," *Renew. Sustain. Energy Rev.*, vol. 57, pp. 111–130, 2016, doi: 10.1016/j.rser.2015.12.099.

[9] D. M. Sackey, M. Amoah, A. B. Jehuri, D. G. Owusu-Manu, and A. Acapkovi, "Techno-economic analysis of a microgrid design for a commercial health facility in Ghana- Case study of Zipline Sefwi-Wiawso," *Sci. Afr.*, vol. 19, p. e01552, 2023, doi: 10.1016/j.sciaf.2023.e01552.

[10] H. Zhu *et al.*, "Online Modelling and Calculation for Operating Temperature of Silicon-Based PV Modules Based on BP-ANN," *Int. J. Photoenergy*, vol. 2017, 2017, doi: 10.1155/2017/6759295.

[11] C. Li *et al.*, "Techno-economic feasibility study of autonomous hybrid wind/PV/battery power system for a household in Urumqi, China," *Energy*, vol. 55, pp. 263–272, 2013, doi: 10.1016/j.energy.2013.03.084.

[12] H. Masrur, M. L. Othman, and S. Member, "Techno-Economic-Environmental Impact of Derating Factors on the Optimally Tilted Grid-Tied Photovoltaic Systems," *Energies*, vol. 4, no. May, pp. 1–22, 2019.

[13] C. Y. Peng, C. C. Kuo, and C. T. Tsai, "Optimal configuration with capacity analysis of pv-plus-bess for behind-the-meter application," *Appl. Sci. Switz.*, vol. 11, no. 17, 2021, doi: 10.3390/app11177851.

[14] WBG, "Climate Change Knowledge Portal." [Online]. Available: https://climateknowledgeportal.worldbank.org/country/cambodia/climate-data-historical

[15] V. Sun, A. Asanakham, T. Deethayat, and T. Kiatsiriroat, "Evaluation of nominal operating cell temperature (NOCT) of glazed photovoltaic thermal module," *Case Stud. Therm. Eng.*, vol. 28, no. August, p. 101361, 2021, doi: 10.1016/j.csite.2021.101361.

[16] IRENA, *Renewable Generation Costs in 2022*. 2022. [Online]. Available: https://www.irena.org/Publications/2023/Aug/Renewable-Power-Generation-Costs-in-2022. [Accessed: Apr. 12, 2024].

[17] L. I. M. Asri, W. N. S. F. W. Ariffin, A. S. M. Zain, J. Nordin, and N. S. Saad, "Comparative Study of Energy Storage Systems (ESSs)," *J. Phys. Conf. Ser.*, vol. 1962, no. 1, p. 012035, Jul. 2021, doi: 10.1088/1742-6596/1962/1/012035.

[18] ADB, "Technical Assistance Consultant ' s Report Regional : Southeast Asia Energy Sector Development , Investment Planning and Capacity Building Facility Cambodia : Energy Transition Sector Development Program," no. October, 2022.

[19] S. Sokrethya, Z. Aminov, N. Van Quan, and T. D. Xuan, "Feasibility of 10 MW Biomass-Fired Power Plant Used Rice Straw in Cambodia," *Energies*, vol. 16, no. 2, 2023, doi: 10.3390/en16020651.

[20] Lazard, "LCOE Lazard," no. April, pp. 1–57, 2023.

[21] D. Eam, V. Vai, C. Chhlonh, and S. Eng, "Planning of an LVAC Distribution System with Centralized PV and Decentralized PV Integration for a Rural Village," *Energies*, vol. 16, no. 16, 2023, doi: 10.3390/en16165995.

[22] V. Viswanathan, K. Mongird, R. Franks, X. Li, V. Sprenkle, and R. Baxter, "Grid energy storage technology cost and performance assessment," no. August, p. 151, 2022.

[23] GDT, "Tax on Income," GDT. Accessed: Apr. 20, 2024. [Online]. Available: https://www.tax.gov.kh/en/content-detail/V61RM1907949992427

[24] Jordan. Stephen, Ross., Randolph, Westerfield., And Bradford, *Fundamental of Corporate Finance*, 12th ed., vol. 4, no. 1. McGraw-Hill, 2019.

[25] GDT, "1005 GDT-Notification on the market interest rate .pdf," GDT. Accessed: Apr. 20, 2024. [Online]. Available: https://www.tax.gov.kh/en/content-detail/mSEtS2775987344711

[26] GDT, "2845 GDT-Notification on the market interest rate .pdf," GDT. Accessed: Apr. 20, 2024. [Online]. Available: https://www.tax.gov.kh/en/content-detail/IVPuA70641178334252

[27] GDT, "5367 GDT-Notification on the market interest rate .pdf." Accessed: Apr. 20, 2024. [Online]. Available: https://www.tax.gov.kh/en/content-detail/hfzDM49441244837457

[28] GDT, "3830 GDT-Notification on the market interest rate .pdf." Accessed: Apr. 20, 2024. [Online]. Available: https://www.tax.gov.kh/en/content-detail/7biAF73208308109271

[29] V. Vai, "Planning of low voltage distribution system with integration of PV sources and storage means - Case of power system of Cambodia," Université Grenoble Alpes, 2017.

[30] NSRDB, "National Solar Radiation Database - Data Viewer," NREL. Accessed: Apr. 10, 2024. [Online]. Available: https://nsrdb.nrel.gov/data-viewer